ADVANCED MATERIALS
www.advmat.de

Engineering Plasmonic Gold Nanostructures and Metamaterials for Biosensing and Nanomedicine

*Yongdong Jin**

The fields of biosensing and nanomedicine have recently witnessed an explosion of interest and progress in the design and study of plasmonic Au nanostructures (p-AuNSs) or metamaterials geared towards a broad range of biological and biomedical applications. Due to their tunable and versatile plasmonic properties, such artificially engineered p-AuNSs and materials have the potential to push biosensor sensitivity towards the single-molecule detection limit, enabling new bioimaging modalities and new analytical techniques and tools capable of single-molecule detection, analysis and manipulation, and to revolutionize the diagnosis and treatment of many diseases, including cancers. This report summarizes and highlights recent major advances in the emerging field of bioapplication-oriented engineering of p-AuNSs and hybrids, focusing on design considerations and ways to carry them out. A brief overview of the optical properties of p-AuNSs is introduced, and then the importance of plasmonic engineering and future promising research directions and challenges in the field are discussed.

1. Introduction

The ability of noble metal nanostructures to manipulate light at the nanoscale and to integrate into biological systems has had great impact in biology and biomedicine.[1–8] Noble metal (plasmonic) nanostructures are capable of confining resonant photons in such a manner as to induce coherent surface plasmon oscillation of their conduction band electrons. Such fascinating plasmon resonance can either radiate light (Mie scattering),[4] or be converted to heat effectively via rapid nonradiative transition (absorption).[4] The mechanisms have been intensively exploited for a variety of innovative bioappications, ranging from biosensing, bioimaging, controlled drug/gene delivery, to photothermal cancer therapy, etc. Compared with non-plasmonic nanostructures, such as semiconductor quantum dots (Qdot) and magnetic nanoparticles (NPs), noble metal nanostructures, especially p-AuNSs have proven to be the most charming platforms suitable for a broad spectrum of bioapplications[3–8] due to their bioinertness and biocompatibility, relatively simple and facile synthetic control and bioconjugation, as well as tunable plasmonic optical properties.

Although Au colloids have a rich history in chemistry[1] and plasmonic effects have been know for more than a century,[9] the substantial biomedical applications of AuNPs started in 1971 with the use of an antibody-AuNP complex for cell surface antigen localization, i.e., the discovery of immunogold labeling by Faulk and Taylor.[10] While intentional plasmonic effect-based applications began in the early 1970s, when Fleischmann[11] and Van Duyne[12] et al. began to study attentively how light scatters from molecules stuck to a (roughened) silver surface and finally revealed a plasmonic effect, i.e., surface-enhanced Raman spectroscopy (SERS). Since then, various p-AuNSs have been extensively studied as SERS-active substrates for sensitive biochemical and materials science studies.[13–15] Building on these foundational and seminal studies, a renaissance of interest in p-AuNSs has occurred subsequently. Especially in the last 10 years, with tremendous advances in both synthetic/nanofabrication methodologies[16–18] and theoretical developments[19–21] in nanostructure plasmonics, the field of biosensing and nanomedicine has witnessed an explosion of interest in the design and study of p-AuNSs geared towards a rich variety of biological and biomedical applications.

Figure 1 highlights landmark breakthroughs and most important developments over the past 10-odd years in the fields. Mirkin et al. pioneered the use of DNA/oligonucleotide as synthons in materials science[22] and developed a number of powerful AuNP-based (ultra)sensitive biodetection schemes[23–27] and gene regulation tools.[28] A solid step towards biomedical applications was taken by Halas et al. in 2003 by using Au nanoshells, a silica core/Au shell NP they invented earlier,[29] for innovative photothermal cancer therapy.[30] Subsequently, various p-AuNSs, including AuNP,[31] nanorod,[32,33] nanocage,[34,35] multifunctional core-shell NPs,[36,38] and Au thin-films,[39] have been extensively exploited for bioimaging,[31,32,36,37,39] controlled drug/gene delivery,[33,35,38] and photothermal cancer therapy.[32,34] The last few years also witnessed rapid development of plasmon rulers (p-rulers) from 1D[40] to 3D.[41]

To exploit fully optical properties of p-AuNSs for desired bioapplications requires the use of both bottom-up and

Prof. Y. D. Jin
State Key Laboratory of Electroanalytical Chemistry
Changchun Institute of Applied Chemistry
Chinese Academy of Sciences
Changchun 130022, Jilin, PR China
E-mail: ydjin@ciac.jl.cn

DOI: 10.1002/adma.201200622

top-down approaches[16–18] to generate structures over length scales ranging from a few nanometers up to a few centimeters. With tremendous developments in nanotechnology over recent decades, scientists have been able to achieve unprecedented control over the sizes, dimensions, morphology, and properties of p-AuNSs. **Figure 2** shows representative p-AuNSs (or metamaterials) and devices synthesized/fabricated that are, and may widely be used for biosensing and nanomedicine. Wet-chemically prepared p-AuNSs, like AuNPs,[5,6,46] nanorods,[47] nanocages,[3,8] and silica/Au nanoshells,[48,49] are the most extensively studied nanostructures in the fields and have been reviewed elsewhere. Discrete nano-gapped Au nanostructures,[50,51] and highly compact multifunctional core-shell NPs[20,37,38,43,52–55] have also been attracting interest due to their enhanced plasmon effects and additional functionalities; While top-down lithographical approaches are a powerful and complementary means to explore a wide range of nanostructures and devices with the advantages of excellent control over size, shape, interparticle spacing, and dimension of surface-bound p-AuNSs.[16–17,21] This type of control is highly important for making reproducible substrate/devices with well-defined complex p-AuNSs,[41,56–66] ranging from dimer- and nanopore-arrays[56,66] to 3D p-rulers.[41]

Although considerable progress has been made recently, it remains challenges to rationally design bioapplication-oriented and powerful p-AuNSs and truly make them clinically relevant. Rather than provide a complete historical survey, I highlight in this progress report recent major advances and milestones in the fields, and focus on ideas and the underlying science rather than details. I first introduce briefly an overview of optical properties of p-AuNSs to outline the basic and most critical design

Yongdong Jin obtained his PhD in Analytical Chemistry from Changchun Institute of Applied Chemistry, the Chinese Academy of Sciences, PR China, with Prof. Shaojun Dong in 2004. He did postdoctoral work at the Weizmann Institute of Science, Israel, with Prof. Mordechai Sheves (jointly with Prof. David Cahen) in 2004-2006, at UCLA with Prof. Yu Huang in 2006-2007, and at the Department of Bioengineering, University of Washington, Seattle with Prof. Xiaohu Gao in 2007-2010. He is presently Professor of Chemistry at the Changchun Institute of Applied Chemistry, Chinese Academy of Sciences. His research interests include plasmonic nanostructures, nanomedicine, energy/nano interface and catalysis, and nanopore-based analytics.

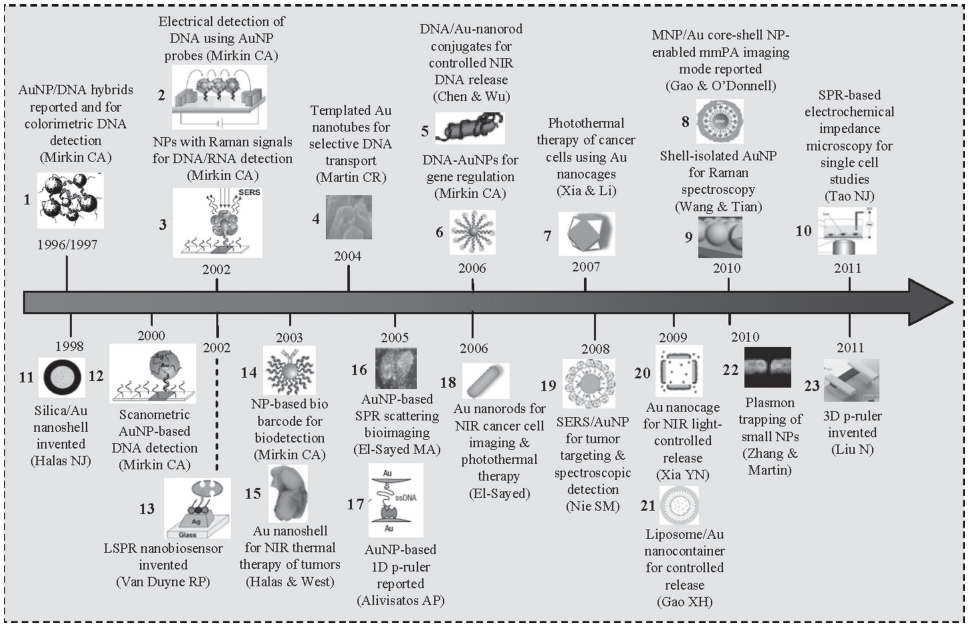

Figure 1. Historical timeline over the past decade of p-AuNSs for biosensing and nanomedicine. 1, reproduced with permission.[22] Copyright 1996, NPG; 2, reproduced with permission.[26] Copyright 2002, AAAS; 3, reproduced with permission.[25] Copyright 2002, AAAS; 4, reproduced with permission.[42] Copyright 2004, AAAS; 5, reproduced with permission.[33] Copyright 2006, ACS; 6, reproduced with permission.[28] Copyright 2006, AAAS; 7, reproduced with permission.[34] Copyright 2007, ACS; 8, reproduced with permission.[37] Copyright 2010, NPG; 9, reproduced with permission.[43] Copyright 2010, NPG; 10, reproduced with permission.[39] Copyright 2011, NPG; 11, reproduced with permission.[29] Copyright 1998, Elsevier; 12, reproduced with permission.[21] Copyright 2000, AAAS; 13, reproduced with permission.[44] Copyright 2002, ACS; 14, reproduced with permission.[27] Copyright 2003, AAAS; 15, reproduced with permission.[30] Copyright 2003, NAS; 16, reproduced with permission.[31] Copyright 2005, ACS; 17, reproduced with permission.[40] Copyright 2005, NPG; 18, reproduced with permission.[32] Copyright 2006, ACS; 19, reproduced with permission.[36] Copyright 2008, NPG; 20, reproduced with permission.[35] Copyright 2009, NPG; 21, reproduced with permission.[38] Copyright 2009, ACS; 22, reproduced with permission.[45] Copyright 2010, ACS; 23, reproduced with permission.[41] Copyright 2011, AAAS.

Adv. Mater. **2012**,
DOI: 10.1002/adma.201200622

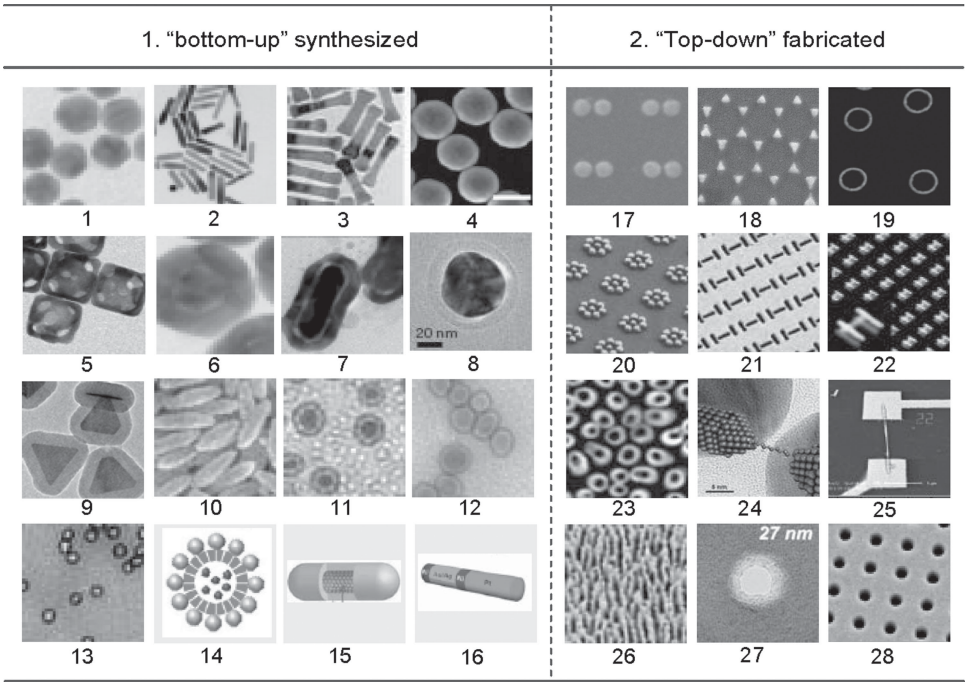

Figure 2. Representative p-AuNSs and devices synthesized/fabricated that are, and may widely be used for biosensing and nanomedicine. 1- Nanosphere. Reproduced with permission.[8] Copyright 2011, RSC; 2- Nanorod. Reproduced with permission.[47]; 3- Nanobone. Reproduced with permission.[67] Copyright 2009, American Chemical Society (ACS); 4- Silica(core)/Au nanoshell. Reproduced with permission.[20] Copyright 2007, ACS; 5-Nanocage. Reproduced with permission.[8] Copyright 2011, Royal Society of Chemistry (RSC); 6-Nanobridged nanogap particle. Reproduced with permission.[50] Copyright 2011, Nature Publishing Group (NPG); 7- Nanorod-in-shell nanostructure. Reproduced with permission.[51] Copyright 2009, ACS; 8- Silica-coated AuNP. Reproduced with permission.[43] Copyright 2010, NPG; 9- Silica-coated Au triangular nanoprism. Reproduced with permission.[52] Copyright 2010, ACS; 10- Hematite/Au nanorice. Reproduced with permission.[20] Copyright 2007, ACS; 11- Qdot/Au core-shell NP. Reproduced with permission.[53] Copyright 2009, NPG; 12- Iron Oxide/Au core-shell NP. Reproduced with permission.[37] Copyright 2010, NPG; 13- liposome/Au nanocontainer. Reproduced with permission.[38] Copyright 2009, ACS; 14- liposome/AuNP assembly. Reproduced with permission.[54]; 15- Golden carbon nanotube. Reproduced with permission.[55] Copyright 2009, NPG; 16- Multisegment nanowire. Reproduced with permission.[68]; 17- Dimer array. Reproduced with permission.[56] Copyright 2009, ACS; 18- Triangular nanodisk array. Reproduced with permission.[57] Copyright 2005, ACS; 19- Nanoring. Reproduced with permission.[58] Copyright 2007, ACS; 20- Oligomer array. Reproduced with permission.[59] Copyright 2011, ACS; 21- Planar metamaterial sensor. Reproduced with permission.[60] Copyright 2010, ACS; 22- Protype of 3D p-ruler nanostructure. Reproduced with permission.[41] Copyright 2011, AAAS; 23- Nanotube array. Reproduced with permission.[61] Copyright 2010, ACS; 24- Nanogap electrodes. Reproduced with permission.[62]; 25- Nanowire field-effect transistor.[63] Copyright 2008, ACS; 26- Nanorod array. Reproduced with permission.[64] Copyright 2009, NPG; 27- Au/SiN nanopore. Reproduced with permission.[65]; 28- Nanopore/hole array. Reproduced with permission.[66] Copyright 2011, NAS. Images have been cropped; see the original papers for scale bars and other information.

principles and considerations, and then illustrate the ways of p-AuNS engineering and their importance and benefits for biosensing and nanomedicine. Finally, some prospects and future research directions are proposed.

2. Plasmonic Properties of Au Nanostructures

P-AuNSs have unique ability to confine resonant photons within their small particle size to induce localized surface plasmon resonance (LSPR) of the conduction band electrons. **Figure 3**a illustrates this phenomenon for a Au nanosphere–the simplest type of LSPR (dipolar LSPR). This plasmonic confinement results in strong light scattering and absorption, and large enhancement of the electric near-field close to the particle's surface (Figure 3b). As a result, all radiative properties or spectroscopic signals from the (bio)molecules at the particle surface, such as light absorption, Rayleigh scattering, fluorescence, and Raman scattering are dramatically enhanced by orders of magnitude; While nonradiative absorption can be rapidly converted to heat (photothermal effect). All these light-particle interactions can be harnessed for biological and biomedical applications.

2.1. Tunable Radiative Properties

The LSPR responses of p-AuNSs–covering from visible to NIR optical window–are sensitive and strongly affected by structural parameters such as size, shape, inter-particle spacing, and the surrounding dielectric environment,[4,21,47] making it the basis for biological labeling, sensing, and detection. For in vivo studies, it is desired to work in the NIR region, especially 650–900 nm, due to the high transmission of tissue blood and water, and hence deeper light penetration (a few centimeters) in this "biological window".[69] Since size–dependent LSPR tunability of solid Au nanospheres is quite limited (and only in the visible

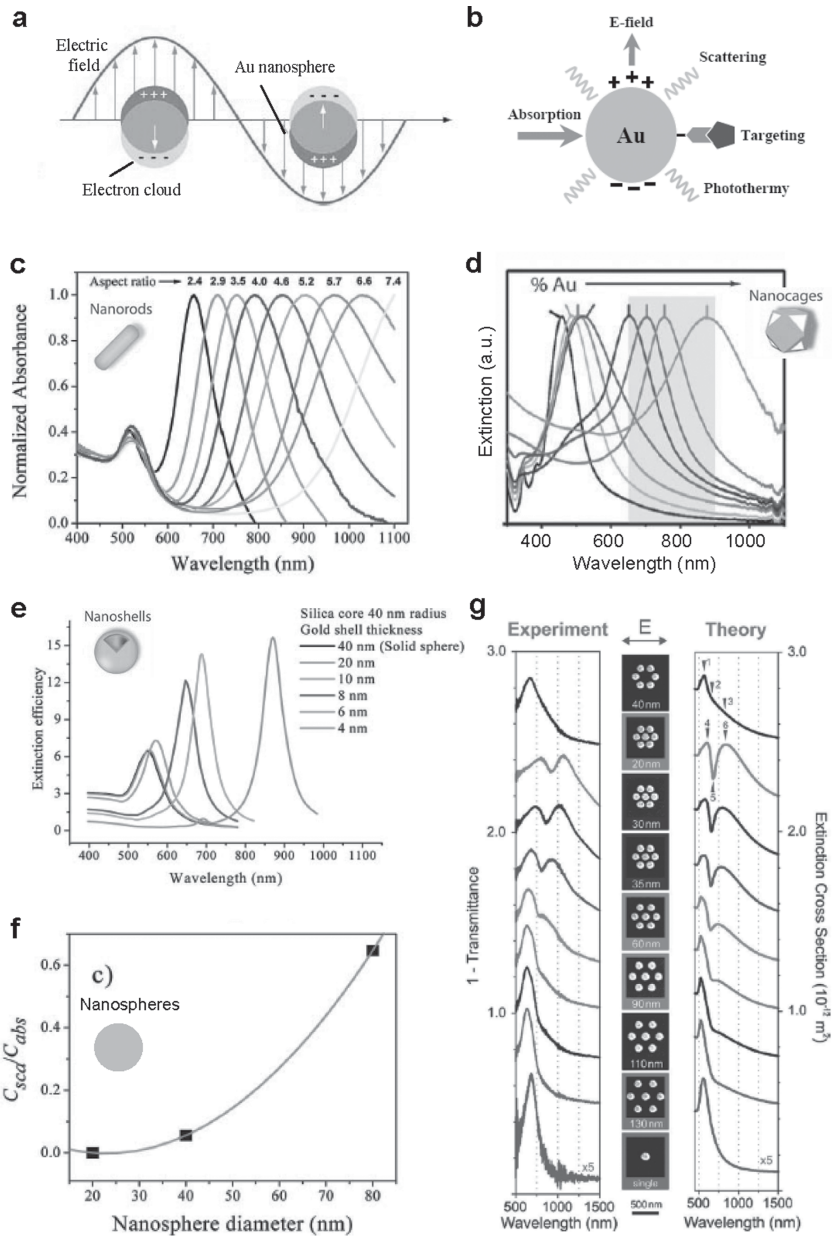

Figure 3. Size-/shape-tunable plasmonic optical properties of various p-AuNSs. a) Schematic illustration of a LSPR of a Au nanosphere showing the collective oscillation of delocalized electrons in response to an external electric field. b) Important optical processes (radiative or nonradiative) resulting from the interaction of light with a AuNPs. c-e) Size, shape, and composition tunability of the LSPR for (c) Au nanorods, (d) Au nanocages, (e) silica core-Au nanoshells, respectively. The NIR tissue transmission window is depicted as a green box in panel (d). f) Increase in the plasmon scattering to absorption ratio by increase in particle volume in Au nanospheres. g) Fano resonances in a variety of lithographically fabricated plasmonic disk oligomers with different NP separations. Panels (c, e, f) reproduced with permission.[4] Copyright 2008, ACS. Panel (d) reproduced with permission.[7] Copyright 2011, RSC. Panel (g) reproduced with permission.[21] Copyright 2011, ACS.

region), the effective ways to tune LSPR into the NIR region is usually by using Au nanorods,[47] nanoshells,[29] and nanocages.[3] As seen from Figure 3c, the long-axis LSPR peak red-shifts from the visible to the NIR as the nanorod aspect ratio increased. Au nanocages (Figure 3d) and nanoshells (Figure 3e) show similar visible-NIR tunability of LSPR by facile control of the wall thickness and void size,[3] and of the shell thickness (or shell thickness-to-core radius ratio) of the particle,[4,29] respectively.

Inter-particle plasmonic coupling occurs when NPs are brought in close proximity to one another. Generally, it does not occur until the edge-to-edge inter-particle separation is less than 2.5 times the particle diameter.[40] El-Sayed et al. proposed a universal relationship between the exponential decay of the spectral shift with respect to inter-particle separation.[70] This relationship is described by the following empirical equation (1):

$$\frac{\Delta\lambda}{\lambda_0} \approx 0.18 \exp\left(\frac{-(s/D)}{0.23}\right)$$

where $\Delta\lambda/\lambda_0$ is fractional plasmon shift and s/D is the separation-to-diameter ratio. This universal scaling law allows for a predictable coupling response from a wide variety of p-AuNSs, including nanospheres, nanodiske, nanoshells, and nanorods, etc.

Note that Mie theory only applies to non-interacting p-AuNSs well separated or present at low concentration in solution. Recent technique advances, however, have allowed the synthesis and fabrication of ordered arrays of (strongly) coupled plasmonic systems[17,21] where the classical electromagnetic description of coupled plasmons is no longer adequate and a quantum mechanical description is necessary to understand their behavior. Halas et al. developed a hybridization model for the plasmon response of complex nanostructures.[19] The theory–an electromagnetic analog of molecular orbital theory, treating p-AuNSs as artificial molecules,[20,71] enables scientists to correctly predict the optical response of complex p-AuNSs of arbitrary shape. Figure 3g shows an example of Fano resonance in a variety of lithographically fabricated plasmonic disk oligomers with different inter-particle separations,[72] clearly illustrating the effect of inter-particle coupling strength on Fano interference. Applying this model as a design principle for p-AuNS fabrication provides a powerful platform for the implementation of optimized plasmonic properties into structures and devices of mesoscale dimensions for desired ultrasensitive biosensing and biomedicine.

2.2. Nonradiative Photothermal Effect

AuNPs absorb and scatter light strongly as a result of the LSPR. The two processes are competing, depending on the particle size and shape.[4] While scattering from a 10 nm AuNP

Adv. Mater. 2012,
DOI: 10.1002/adma.201200622

is negligible, the relative contribution of scattering increases rapidly with increase in the particle volume (Figure 3f). Ultrafast laser spectroscopic studies[4,73] have established that the absorbed light is converted to heat efficiently at the rate of ~1 ps by rapid electron-phonon and phonon-phonon processes. At very fast rates of energy deposition relative to lattice cooling, the photothermal heating can result in the ablation of the NP or desorption of surface-capping, or it may melt or reshape the NP (~30 ps).[4] At slower rates, the lattice cools via phonon-phonon process (~100 ps) leading to heating of the local environment (surrounding medium). The highly efficient and localized light-to-heat conversion by p-AuNSs makes them very useful for gene/drug delivery[33,35,38] and photothermal therapy of cancers and other diseases.[30,32,34] Due to high adsorption cross sections (e.g., 10–50 nm AuNPs offer 5 or more orders of magnitude larger absorption coefficients compared with conventional dyes), it requires only minimal irradiation energy to achieve cell destruction, making therapy minimally invasive.[4] The laser power density threshold for selective destruction of cancer cells for Au nanoshells, nanorods, and nanocages, are ~35, 10, and 1.5 W/cm^2, respectively.[34] In vivo studies[30] under magnetic resonance guidance revealed that exposure to low doses of NIR light (820 nm, 4 W/cm^2) in solid tumors treated with Au nanoshells reached average maximum temperatures capable of inducing irreversible tissue damage (ΔT = 37.4 ± 6.6 °C) within 4–6 min (versus ΔT < 10 °C in controls treated without Au nanoshells).

Another paradigm of photothermal bioapplication would be the use of p-AuNSs for photoacoustic (PA) imaging (or called PA tomography, PAT).[74–76] PA imaging is based on the PA effect, where absorption of pulsed laser radiation results in transient heat. The resulting thermo-elastic expansion generates an acoustic signal, which can be directly measured. So far, Au nanoshell,[75] nanocage,[76] and golden carbon nanotubes,[55,77] have been successfully used as contrast-enhancing agent for in vivo PAT of Rat brain (cerebral cortex),[75,76] and for in vivo multiplex PA detection of circulating tumor cells.[77]

2.3. Plasmon Near-Field and Optical Force

Conventional far-field optical tweezers, formed at the diffraction-limited focus of a laser beam, have become a powerful tool for manipulating micrometer-sized objects, but failed for trapping nanometer-sized objects. P-AuNSs, due to strong near-field enhancement and the ability to control light at the subwavelength scale, are gaining attention for the plasmonic trapping of small NPs and biological nano-objects.[78] Volpe et al. used photonic force microscopy to probe the SPP force field and measured a 40-fold enhancement to the force magnitude.[79] Martin et al. have recently managed to trap 10 nm AuNPs using plasmonic dipole antennas and recorded optically single NP trapping events in real time.[45] The capability of trapping, ultra-accurate positioning and manipulation of single nano-objects,[80] along with easy system integration, make the plasmonic trapping technique promising for single-particle/-biomolecule sensing, studies and manipulations.

3. Why Plasmonic Engineering?

Plasmonic engineering (P-engineering) we referred to herein is any means of fine-manufacturing nanostructures with flexible and precise control over size, shape and inter-particle spacing down to (a few) nanometer scale and with desired plasmonic properties. As the field of plasmonics grows, new synthesis, fabrication and characterization methods for p-AuNSs have advanced to a point that deliberate engineering of their surface, size, shape, and pattern is possible, thereby allowing exquisite control of their properties and system integration, and boosting innovative researches in biomedical applications.

3.1. Design Considerations and Strategies

Applying p-AuNSs for bioapplications requires the understanding of various nano/nano-interface and nano/bio-interface involved,[81] and the use of well-established experimental structure-property relationships and theoretical simulations for nanostructure preparations. The ideal p-AuNSs are envisioned with desired plasmonic properties and functionality, capable of surmounting biological barriers encountered, and having the potential to revolutionize the diagnosis and treatment of many diseases. Strategies so far in the direction (**Figure 4**) include: (1) size-/shape-controlled wet-chemical synthesis–fine-tuning size-/shape-dependent optical and photothermal properties for desired in vitro/in vivo bioapplications; (2) "top-down" nanolithographic fabrication–creating more advanced and versatile p-AuNSs and devices unavailable by "bottom-up" methods that are powerful for ultrasensitive biosensing/detections, etc.; (3) inter-particle distance/gap design and molecular-/nano-engineering–manipulating plamonic near-field coupling and Fano resonance of tailor-made complex nanostructures on the nanoscale for gentle and ultrasensitive biosensing/bioassy down to molecular level; (4) integrated P-engineering of multifunctional nanostructures–creating uniform and highly impact "all-in-one" hybrid p-AuNSs with integrated multifunctionality for multimodal imaging and especially for cancer theranostics.

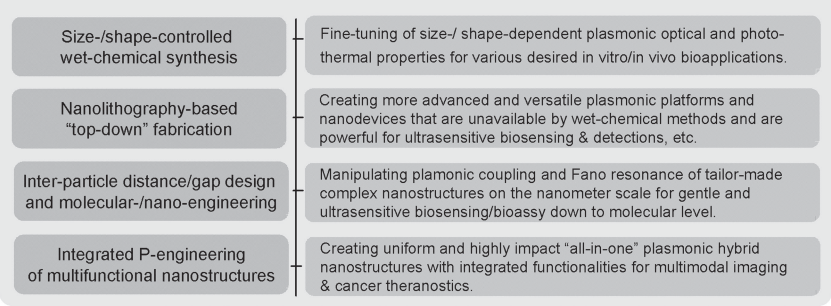

Figure 4. Ways and benefits of P-engineering Au nanostructures for biosensing & nanomedicine.

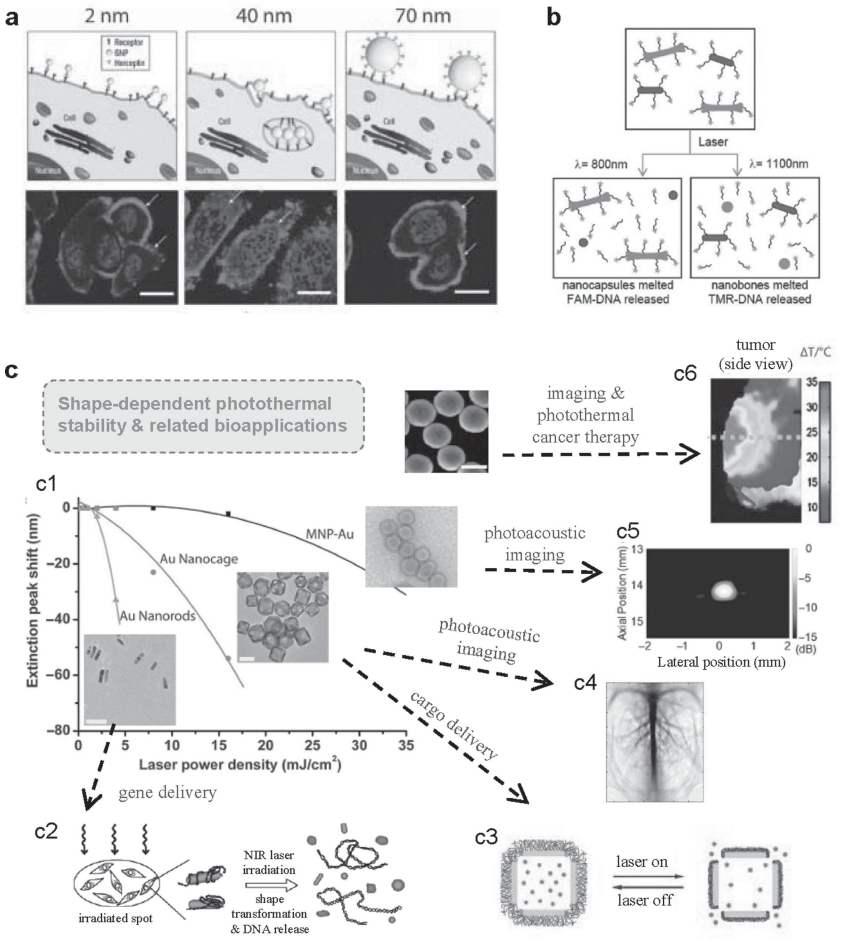

Figure 5. Size and shape of p-AuNSs matter. a) Schematic illustration how size and receptor density of antibody-AuNP conjugates affect EGFR-mediated uptake of Herceptin-labeled AuNPs into SK-BR-3 breast cancer cells. 2 nm AuNPs were not efficiently internalized because multiple receptors could not be simultaneously bound. 70 nm particles exhibited multivalent binding, however they were too large for efficient membrane wrapping (i.e. endocytosis). Reproduced with permission.[85] Copyright 2008, NPG. b) Schematic overview of selective release of multiple DNA oligonucleotides from Au nanorods. Laser irradiation of DNA-conjugated nanocapsules (dark ovals) and nanobones (gray bones) are exposed to λ_{800} irradiation (left), which melts the nanocapsules and selectively releases the conjugated DNA (labeled by FAM (gray triangles)). Exposure to λ_{1100} irradiation (right) melts the nanobones, selectively releasing the conjugated DNA (labeled by TMR (gray stars)). Reproduced with permission.[67] Copyright 2009, ACS. c) Selected examples of shape-dependent photothermal stability and related bioapplications of p-AuNSs. Au nanorods with relatively poor photostability are preferred as platforms for light-controlled drug/gene delivery, whereas Au nanocages with medium stability are suitable for both cargo delivery and in vivo optical imaging. The silica/Au nanoshells with thicker Au layers are more tolerable for in vivo imaging and photothermal cancer therapy. Schemes and Figures (C1-C6) reproduced with permission.[8,30,33,37,76] Copyright 2010, NPG (C1); 2006, ACS (C2); 2011, RSC (C3); 2007, ACS (C4); 2010, NPG (C5); 2003, NAS (C6).

3.2. Size, Shape, and Distance Matter

The size of AuNP dictates not only particle's optical properties but also the effectiveness/fate of its bioapplications. Since the absorption dominates the extinction (absorption + scattering) spectrum for smaller AuNPs while the relative contribution of scattering increases rapidly with increase in the NP size (cf. Figure 3f), AuNPs with diameter smaller than ~40 nm are typical used for absorption-based bioassays, whereas bigger NPs are preferred for scattering-based biosensing and dark-field imaging. While particles with medium diameter of ~40–80 nm were suitable for photothermal drug/gene delivery and cancer therapy due to a compromise between their optical properties and size effects. The ideal sizes of therapeutic NPs should be in the range of 10–100 nm, as larger particles have limited diffusion in the extracellular space[82] while particles less than 5 nm are rapidly cleared from the circulation through extravasation or renal clearance.[83]

The size effects of p-AuNSs on cellular behavior and cytotoxicity have been studied recently with nanosphere as an example mostly. Chan et al. have investigated the intracellular uptake of different sized AuNPs, revealing that kinetics and saturation concentrations are highly size-dependent (e.g., uptake half-life of 14, 50, and 74 nm NPs is 2.10, 1.90, and 2.24 h, respectively).[84] They investigated also the cellular response to herceptin-coated 2–100 nm AuNPs and found that 40 and 50 nm particles have the greatest effect on cell signaling functions (**Figure 5**a).[85] Simon et al. examined 0.8-15 nm AuNPs stabilized by triphenylphosphine derivatives. In their case, 1.4-nm particles were highly toxic, whereas 15-nm-diameter particles were nontoxic, even at up to 100-fold higher concentrations.[86] The size effect of Au nanorods with different aspect ratio have also be exploited for controlled multiple-drug delivery,[67] in which two different DNA oligonucleotides were loaded on two different Au nanorods and selective DNA releases were induced by selective melting of Au nanorods via ultrafast laser irradiation at the nanorods' longitudinal SPR peaks (Figure 5b).

The shape of p-AuNSs (like nanorods/cages) could also influence cellular uptake.[84,87] Since nanoprobe's photo-stability is directly linked with particles' imaging capability and therapeutic effects, the most fascinating aspect would be the shape-dependent photostability of p-AuNSs and their selectively optimal bioapplications accordingly, as illustrated in Figure 5c. Compared with Au nanorods and nanocages, Fe_3O_4/Au core-shell NPs exhibited remarkable stability under identical laser irradiation.[37] The laser fluence threshold for nanoprobe degradation for Au nanorods, nanocages, and Fe_3O_4/Au core-shell NPs are ~2, 6, and 15 mJ cm^{-2}, respectively, indicating superb PA imaging capability of the latter.[37] Above these fluences, significant SPR peak shifts were observed indicating nanoprobe degradation. Therefore, Au nanorods with relatively poor photostability are preferred as platforms for light-controlled drug/gene delivery,[33,67] whereas Au nanocages with medium stability are suitable for both cargo delivery[35] and in vivo optical imaging.[76] The silica/Au nanoshells with thicker

Adv. Mater. 2012,
DOI: 10.1002/adma.201200622

Au layers, due to better photostability, will be more tolerable for in vivo imaging and photothermal cancer therapy.[30]

The inter-particle spacing/distance as aforementioned, is another crucial parameter for plasmonicly coupled nanostructures[20,21,40,41] and has provided a strong basis of p-AuNSs for applications in ultrasensitive biosensing[17,23,40,41] and sophisticated SERS studies.[50,88]

3.3. Multifunctionality

One of the ultimate goals of P-engineering is aimed at integrated synthesis of compact "all-in-one" nanostructures, by combining multiple discrete functional components (plasmonic and non-plasmonic) into a single nanostructure, with combined/desired functions.[37,53] As for imaging nanoprobes, the complementary ability of different imaging modalities could be harnessed to great effect by using them in tandem[89] since each type of individual nanoprobe displays distinct advantages and limitations.[37] For example, magnetic NPs have become an important contrast agent in T2-weighted magnetic resonance imaging (MRI) because MRI offers high resolution and excellent tissue penetration depth. However, MRI is not as sensitive as optical imaging or positron emission tomography, and is difficult to visualize in microscopic tissue examination.[90] Multimodal MRI-optical imaging contrast agents, therefore, show promising for clinic uses by combining the high spatial and temporal resolution of MRI with the sensitivity of the optical imaging probes.

Highly-integrated multifunctional "all-in-one" p-AuNSs with combined targeting, diagnostic and therapeutic functions[49] will enable the capabilities to perform multiple parallel tasks, and provide a platform onto which image-guided therapeutic technologies can be developed for the targeted imaging and theranostic of cancers.[91] A major challenge in the field is how to engineer nanoprobes with integrated or even created functionalities[37] while still maintaining compact sizes.[92]

4. Recent Advances and Highlights in Plasmonic Engineering

4.1. Surface Molecular Engineering

Surface engineering of AuNPs with ligands and biomolecules (DNA, protein, etc.) is important for a broad range of bioapplications, in which the NP-(bio)molecular interactions and conjugations play a central role.[5,6,46] A recent report[93] highlighted the role of surface ligand structure and order in cell-membrane penetration by particles (**Figure 6**a). In the study, AuNPs (~6 nm) were modified with

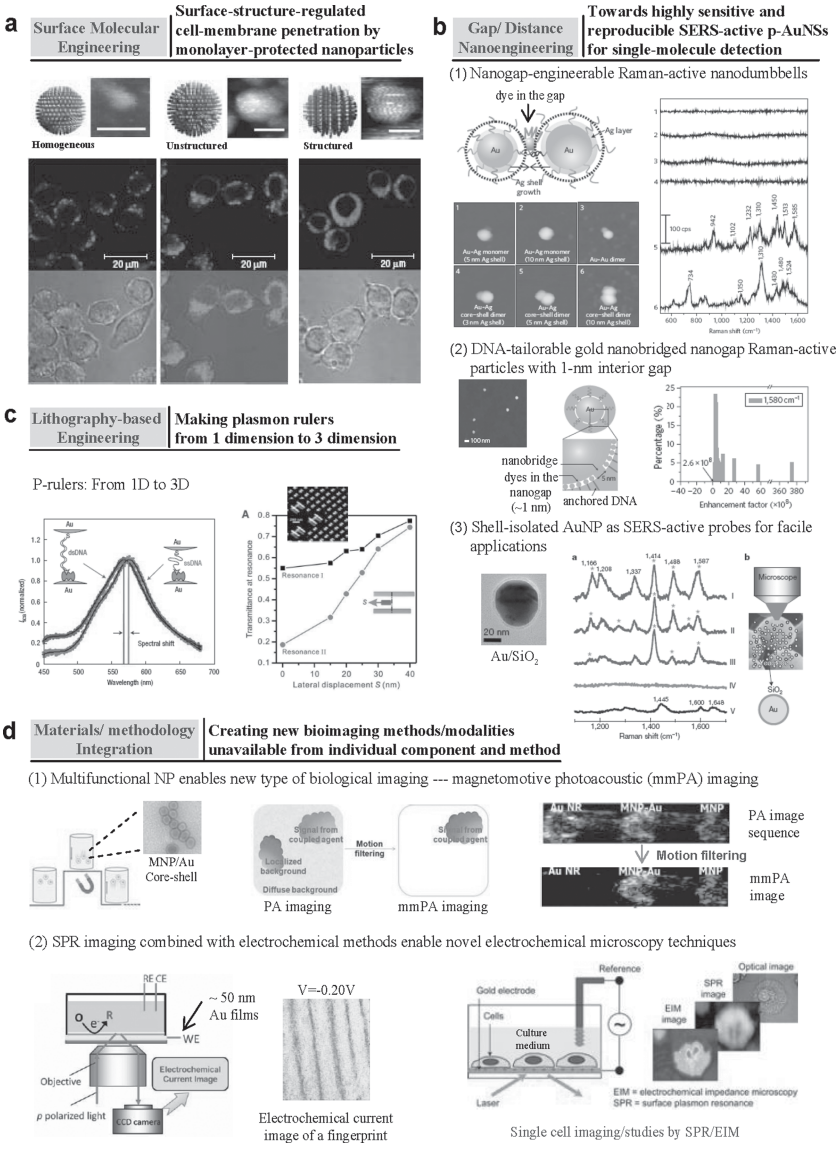

Figure 6. Ways and benefits of p-AuNS engineering for biosensing and nanomedicine. a) AuNPs with ordered arrangements of hydrophilic and hydrophobic surface functional groups exhibit altered patterns of subcellular localization in cells. Schematic diagrams (top panels) of the ligand shell structure of the NPs and representative STM images (scale bars 5 nm). BODIPY fluorescence (middle panels) and bright-field/fluorescence overlay (lower panels) images of dendritic cells incubated with 0.2 mg mL^{-1} of MUS, 66-34 br-OT or 66-34 OT NPs (from left to right) for 3 h in serum-free medium at 37 °C. See the original paper for details. Images reproduced with permission.[93] Copyright 2008, NPG. b) Three examples of gap/distance nanoengineering towards highly sensitive and reproducible SERS-active nanostructures for single-molecule detection. Images reproduced with permission.[43,50,88] Images 1,2,3 copyright 2010, 2011, 2010 respectively, NPG. c) Lithography advance make the development of plasmon ruler from 1D to 3D possible. Image reproduced with permission.[40,41] Images 1,2 copyright 2005 NPG, 2011 AAAS, respectively. d) Two examples of materials/methodology integration that enables new bioimaging methods/modalities unavailable from individual component and method. Images reproduced with permission: 1[37] Copyright 2010, NPG; 2[39,94] Copyright 2010 AAAS, 2011 NPG, respectively.

a shell of alternating hydrophobic and hydrophilic ligands. The well-organized striped particles were able to penetrate cell membranes at 37 and 4 °C without notable evidence of membrane disruption, whereas the other coated with the same moieties but in a random distribution were mostly trapped in endosomes.

Surface charge control[95] and supramolecular chemistry[96] were recently proved as two powerful tools to regulate biological processes for drug delivery and therapeutic applications. Forbes et al.[95] showed that AuNPs carrying either fluorescein or doxorubicin molecules move and localize differently in an in vitro 3D model of tumor tissue, depending on whether the NPs are positively or negatively charged. The experimental/theoretical results indicate that positive particles may be more effective for drug delivery because they are taken up to a greater extent by proliferating cells; While negative particles, diffusing more quickly, may perform better when delivering drugs deep into tissues. Rotello et al.[96] demonstrated that engineering of host-guest systems to function inside the cell provides a potential powerful supramolecular strategy for the regulation of therapeutics. They presented a host-guest system featuring diaminohexane-terminated AuNPs (AuNP-NH(2)) and complementary cucurbit[7]uril (CB[7]) that form a non-toxic assembly that is readily taken up by the cells. Intracellular triggering of the therapeutic effect of AuNP-NH(2) was then achieved through the administration of 1-adamantylamine (ADA), removing CB[7] from the NP surface, causing the endosomal release and concomitant in situ cytotoxicity of AuNP-NH(2).

4.2. Gap/Distance Nanoengineering

Lithographic methods are by far widely used for the production of surface-bound p-AuNSs with unparalleled control over the size, shape, inter-particle spacing, and alignment.[17] Various p-AuNSs with well-defined inter-particle gap/distance (see Figure 2), such as dimer array,[56] triangular nanodisk array,[57] oligomer array,[59] planar metamaterial sensor,[60] 3D p-ruler,[41] nanogapped electrode,[62] and nanopore/hole array,[66] etc. have been lithographically fabricated. The major drawback, however, is that p-AuNSs with dimensions less than 10 nm are not readily obtainable.[47]

Bottom-up solution-phase synthesis therefore is an alternative to fine control p-AuNSs on a few-nm scale.[17,40] Gao et al.[37,53] exploited layer-by-layer self-assembly technique to create a few-nm-thick dielectric layers (gap) sandwiched between two inorganic materials, and succeeded in the production of multifunctional, polymer-gaped Qdot/Au,[53] and Fe_3O_4/Au core-shell NPs.[37] Aiming to prepare reproducible, high-performance SERS-active p-AuNSs, three intriguing strategies (Figure 6b) based on gap/distance nanoengineering have been explored recently.[43,50,88] Nam, Suh et al. reported[88] a high-yield synthetic strategy to obtain gap-tailorable Au/Ag core-shell nanodumbbells (GSNDs) via controlled Ag shell growth on the surface of the single-target-DNA hybridized AuNP heterodimers. The authors[50] also used DNA-modified AuNPs as seeds to synthesize in high yield a new class of nanostructures (termed Au nanobridged nanogap particles, Au-NNPs) with a well-defined, hollow, 1 nm interior gap between a Au core and a Au shell. Wang and Tian et al.[43] engineered nanoscale separations between AuNP and SERS active sites by controllable coating AuNPs with an ultrathin silica or alumina shell. The ultrathin coating keeps the NPs from agglomerating, separates them from direct contact with the probed material and allows the NPs to conform to different contours of substrates, making the NPs promising for practical applications of SERS.

4.3. Multifunctional Hybrid Core-Shell p-AuNSs

Integrated synthesis of "all-in-one" p-AuNSs, in particular compact core-shell structures,[37,38,49,53,55,91] is a current pursuit. Retaining unique properties, especially optical and electrical properties, of each component after nanoscale integration is, however, a long-standing problem. It is particularly difficult when combining fluorescent semiconductor Qdot with p-AuNSs in the core-shell format, because Au can quench the fluorescence and conventional Au nanoshell formation methods failed in producing very thin and smooth Au layers.[29,97] Gao et al.[53] developed a biomimetic tactics for controlled deposition of very thin (~2–4 nm) and smooth Au layers by using surface-assembled poly-L-histidine monolayer as templates, and addressed quenching problem by creating a polymer (dielectric) gap between the Qdot core and Au shell with nanometer precision through layer-by-layer assembly. The approach provides a general route for the deposition of ultrathin Au layers onto virtually any discrete core nanostructure. And in doing so, it is easy to tune LSPR response of the resulting compact hybrid NPs into NIR region,[37] which is desirable for potential in vivo applications. The authors extended the approach to prepare Fe_3O_4/Au[37] and liposome/Au[38] core-shell NPs, and succeeded in their use as multimodal imaging contrast agents[37] and NIR light-controllable drug delivery vehicles.[38] More importantly, the magnetic plasmonic Fe_3O_4/Au core-shell NPs enable a new biological imaging mode, magnetomotive photoacoustic (mmPA) imaging.[37]

5. Developments and Benefits for Bioapplications

5.1. (Ultra)sensitive Biosensing

The LSPR frequency (wavelength), either by absorption or scattering, depends on the inter-particle spacing and the dielectric constant (i.e., refractive index, RI) of the medium surrounding the particle, and provides basis for biosensing.[44,98] Typical biosensing schemes using AuNPs are based on distance-dependent particle-particle coupling,[23] and Rayleigh scattering.[24,25,27] The sensitivity, defined as the plasmon shift per RI unit (RIU) change ($d\lambda_{SPR}/dn_m$), depends on the shape of the NPs.[4,47] Therefore, NP geometry can be readily tuned to enhance plasmonic sensitivity: typically anisotropic NPs (like nanorods, nanoshells, and nanoprisms) give higher sensitivity than nanospheres.[4,47] Au nanospheres of 30-nm-diameter offer a modest sensitivity of ~70 nm/RIU,[4] whereas Au nanoshells or nanocages offer enhanced sensitivity. With decreasing shell thickness (relative to silica core size), there is near-exponential increase in the plasmon sensitivity, for example, from 129 to 363 nm/RIU with variation in shell thickness from 40 to

Adv. Mater. 2012,
DOI: 10.1002/adma.201200622

4 nm.[4] The silica-encapsulated Au nanoprisms have sensitivities as high as 737 nm/RIU.[52] Lithographically fabricated p-AuNSs or metamaterials, such as dimmers,[56] nanotubes,[61] nanorods,[64] nanoholes,[66] disks,[99] and nanorings[58] arrays, and more complex metamaterials[60] due to the tunability of higher dielectric sensitivity, show promising for ultrasensitive biosensing.[56,58,60,61,64,66,99] For example, extremely sharp Fano resonances in high-quality nanohole sensors enable seeing single biomolecular monolayers with naked eye;[66] Benefiting from a substantial overlap between the probing field and the active biological substance incorporated between the arrayed nanorods and a strong plasmon-mediated energy confinement inside the layer, the Au nanorod metamaterial provides very high sensitivity of more than 30 000 nm/RIU and a large probe depth (500 nm).[64] Käll et al.[100] utilized a combination of LSPR sensing and enzymelinked immunosorbent assay to develop a simple colorimetric biosensing methodology with single molecule sensitivity, in which the surface-localized horseradish peroxidase (HRP) enzymatic reaction dramatically amplifies the shift of the LSPR scattering maximum.

Special p-AuNSs like artificial nanopores (or nanoholes, including nanotubes) have also attracted increasing attention recently as the sensing elements in biosensors.[42,65,101–104] By monitoring ion currents and forces as (single) molecules pass through a solid-state nanopore, it is possible to investigate a wide range of single-molecule phenomena involving DNA, RNA and proteins.[102,103] Plasmonic Au nanopore sensors, due to additional plasmonic functions, could one day revolutionize biosensing, but further technological challenges including methodology/device integration remain before this promise is realized. Another attractive special p-AuNSs-based ultrasensitive biosensing platform is the nanowire- or nanogap-based label-free nanoelectronic detections. The first nanoelectrical protein detection was reported by Lieber group[105] using single p-type silicon nanowire devices in 2001. Electrical detection of DNA array using AuNP probes in an electrode gap was reported in 2002 by Mirkin et al.[26] The method can detect target DNA at concentrations as low as 500 femtomolar. Nanogapped Au electrodes[106,107] and multisegment nanowire-based field-effect transistors[63] were also exploited for glucose sensing,[106] DNA detection,[63] and conductance measurement of single DNA molecules.[107] Due to the small size of the nanojunction, the enzyme is regenerated naturally without the need of redox mediators, which consumes minimal amount of oxygen and gives very fast response (<200 ms). These features make it potentially useful for in vivo glucose detection.[106] Recently, Taniguchi et al.[104] developed a self-alignment technique, by combination of nanopore analytics and electrical detection, to form a nanopore-nanoelectrode device consisting of a sub-nanometer electrode gap in a 15 nm-sized SiO_2 pore. They performed electrical identification of nucleobases in a DNA oligomer, thereby suggesting the potential use of this integrated device for label-free electrical DNA sequencing.

5.2. Plasmon Ruler Evolved from 1D to 3D

P-rulers can be used to determine nanoscale distances within chemical or biological species. The first generation (1D) p-rulers consisting of a single pairs of Au- and Ag-NPs,[40] are based on the spectral shift of the scattering spectrum when two NPs approach one another (Figure 6c). The equation 1[70] is useful in the determination of intersite distances in biological systems using p-rulers. As compared to the Förster (fluorescence) resonance energy transfer (FRET)-based distance probes, the p-rulers do not blink or bleach and therefore, measurements can be made continuously over long periods of time. While the FRET ruler has a maximum range of 10-nm due to the steep $1/R^6$ dependence between two molecular species, the p-ruler range is much larger, e.g. 70-nm for a dimer of 40-nm AuNPs, and can be increased directly by increasing the particle dimension.[40] NP pair p-rulers linked by ss-DNA[40] or ds-DNA[108] have shown to be able to study the kinetics of single DNA hybridization events[40] and used for real-time measuring nuclease activity and DNA footprinting.[108] An average wavelength shift of approximately 1.24-nm was observed per DNA base pair.[108]

The 1D p-rulers, however, hampers the comprehensive understanding of many intriguing 3D processes in biological and soft matter. Liu et al.[41] demonstrated a 3D p-ruler based on coupled plasmonic oligomers in combination with high-resolution plasmon spectroscopy. They used a stack of five Au nanorods (in an 'H' arrangement) that can report not just a single distance but the precise position of one central rod with respect to the others (Figure 6c). Therefore, the 3D ruler offers measurements additional degrees of freedom, such as rotating, twisting, tilting and any conformational changes. Such rulers will be useful for investigating dynamic process of single or complex macromolecular in physiological environments, and could one day be used to improve understanding of protein folding and interactions and help defeating protein-based diseases like Alzheimer's and Parkinson's disease.

5.3. SERS Goes Reproducible and Fine-Tunable

Since its discovery,[11] SERS has been extensively used and reviewed from fundamental mechanisms to biomedical applications.[12,13,15,109,110] Its commercialization, however, has been hampered in many areas by difficulties in achieving highly accurate control over the surface nanostructures and the reproducibility. An ideal SERS nanostructure should induce a high signal enhancement, generate a reproducible and uniform response, and should be easy to synthesize and use. Recent attempts toward this end made SERS-active p-AuNSs reproducible and practically useful[43,50,88] (Figure 6b). As reported, the individual gold-silver core-shell nanodumbbells (GSNDs)[88] have single-DNA sensitivity with high structural reproducibility; the enhancement factors of Au-NNPs (Au nanobridged nanogap particles) were narrowly distributed between 1.0×10^8 and 5.0×10^9 with SERS signals down to 10 fM concentrations,[50] which is sufficient for single-molecule detection; While the effectiveness and simplicity of the shell-isolated NP-enhanced Raman spectroscopy (SHINERS)[43] expand significantly the flexibility of SERS for practical applications. Recently, Nie group[36] developed a new class of robust SERS tags of pegylated NIR-emission dye molecules adsorbed onto AuNPs, and applied them for SERs detection of tumors in mice. This study advanced the

development of SERS from bench to in vivo applications and offered the possibility for future SERs-based clinical cancer diagnosis.

5.4. Multifunctional p-AuNSs for Cancer Nanotechnology and Theranostics

Multifunctional p-AuNSs or hybrids, due to their functional versatility and properties unique from both their parent molecules and their particle scaffolds, can exhibit high biocompatibility, increased binding affinity/targeting selectivity, low immunogenic responses and long circulatory half life, rapid transport kinetics, and size-dependent/-enhanced tumor uptake. These properties combined with their tunable NIR optical properties make them promising as imaging contrast agents and next-generation anticancer agents.[7] The p-AuNSs and hybrids to date, including AuNP[31,95,96] and AuNP assemblies,[111] nanoshell,[30,112] (hybrid) nanorod,[32,33,113] nanocage,[34,35] multifunctional core-shell NP,[36] and golden carbon nanotube[55] etc., have been extensively exploited for cancer-targeting imaging,[31,32,36,55] controlled intracellular drug/gene delivery,[33,35,95,96,112–115] photothermal cancer therapy,[30,32,34,51] and early diagnosis[77] and inexpensive and non-invasive diagnosis of cancer.[111] Recent studies focus on the combination of diagnostic detection, targeting imaging, with therapeutic functions within an integrated "all-in-one" single nanocomplex.[49] Such theranostic nanoprobes can simultaneously deliver diagnostic and therapeutic functions, enabling concomitant detection and localized treatment of cancer (and other diseases) in a single procedure. For example, multifunctional (Au) nanoshells,[91] constructed by coating a Au nanoshell with a silica epilayer doped with Fe_3O_4 and the fluorophore ICG, were recently examined as a multimodal theranostic nanoprobe for enhanced NIR fluorescence and MRI imaging and for targeted photothermal ablation of cancer cells, showing theranostic potential for imaging subcutaneous breast cancer tumors in animal models and the distribution of tumors in various tissues. Such theranostic agents should ultimately allow us to simultaneously visualize and deliver therapeutics to metastatic cancer sites[116] and early detection of circulating tumor cells.[77] Advances in the field will enable theranostics to transition from the laboratory to clinical settings.[117]

5.5. Integration Enables New Bioimaging Modality

Engineering compact multimodal imaging nanoprobes will have profound impact on molecular diagnostics, imaging and therapeutics, and it is highly desirable to enable new imaging modes not available from each individual component for enhanced contrast specificity. One successful example is the use of multifunctional Fe_3O_4/Au core-shell NPs (<40 nm) for multimodal imaging.[37] Due to the combination of NIR optical absorption and magnetic response, the imaging nanoprobes can be used for PA imaging and can erase the background noise by using a pulsing magnetic field to shake the NPs and used image processing techniques to remove everything except the vibrating pixels. It, therefore, enables a new bioimaging mode, magnetomotive photoacoustic (mmPA) imaging, with remarkable contrast enhancement compared with PA images using conventional NP contrast agents (Figure 6d(1)). The inexpensive, non-invasive, and high spatial resolution and deep tissue penetration nature of the PA imaging modality, together with the background eliminating capability, make the new imaging technique very sensitive and promising for clinical uses and envisioned could one day 'see' single cancer cells in vivo. And potentially, it can be easily combined with photothermal cancer therapy, because both techniques share similar mechanisms.

Another successful example is the new developments in SPR imaging technique. Optical SPR imaging is powerful for in situ real-time characterization of Au/dielectric interfaces and has been widely used for biomolecule interaction studies. In practice, a ~50 nm-thick Au thin-film deposited on a glass substrate by either vacuum deposition/sputtering or a wet-chemical way,[118] is used for the excitation of SP modes in the common Kretschmann configuration. Tao et al.[39,94] advanced recently new SPR imaging techniques by methodology integration. They demonstrated an electrochemical microscopy technique based on the detection of variations in local electrochemical current from optical signals arising from SPR.[94] Since the imaging technique is noninvasive, scanning-free, fast, and the signal varies with current density rather than current, it enables local electrochemical measurements (e.g. voltammetry and amperometry) with high spatial resolution and sensitivity (Figure 6d(2), left panel). The authors combined technically also electrochemical impedance spectroscopy (EIS) with SPR imaging and extended for single cell imaging and studies.[39] The new technique uses SPR to detect impedance optically. It, therefore, resolves local impedance with submicrometer spatial resolution, and was used to monitor the dynamics of cellular processes (apoptosis and electroporation of individual cells) with millisecond time resolution. In addition to the electrochemical impedance microscopy (EIM) image, the new technique produces simultaneous optical and SPR imagery, providing useful complementary information (Figure 6d(2), right panel). The technique would be capable of resolving many subcellular structures and processes (such as ion channel activities and drug-cell interactions) without labels, and with excellent detection sensitivity, offering fresh insights into previously elusive cellular features and events.

6. Conclusion and Outlook

Due to their biocompatibility and tunable surface chemistry, morphology, and unique optical properties of p-AuNSs, the fields of biosensing and nanomedicine have recently witnessed an explosion of interest in the use of a variety of accurately engineered p-AuNSs for various bioapplications ranging from ultrasensitive biosensing, imaging, controlled drug/gene delivery, to photothermal cancer therapy. As a result, we now have a better understanding on how we can accurately design and optimize plasmonic (and multifunctional) properties of (hybrid) p-AuNSs for a specific bioapplications. It must, however, be acknowledged that the biomedical promise of p-AuNSs has so far mainly been based on proof-of-concept demonstrations. It therefore remains a significant challenge to rationally design more powerful and

Adv. Mater. 2012,
DOI: 10.1002/adma.201200622

applicable p-AuNSs that can fulfill the requirements for bioapplications, and find practical ways to use and integrate them with real-life clinic settings and applications.

The impact of p-AuNSs in biology and biomedicine is, however, determined not only by their biomedical merits, but also by the new functions and means that be created capable of probing fundamentally previously unknown biological world and events down to single cell or molecule level. In this regard, multifunctional "all-in-one" p-AuNSs show continued growing interest in cancer nanotechnology and theranostics; While a couple of special p-AuNSs enable powerful new techniques, but currently there will be hurdles for practical applications. For instance, 3D p-rulers,[41] though promising to measure 3D position of nano-objects, it is challenging to find facile fabrication methods and realize such function in real biological and soft-matter systems. Although lithography method is superior for preparing complex objects such as 3D p-rulers, bottom-up synthesis of complex p-AuNSs as 3D p-rulers (and their incorporating into biochemical systems) would be the next competition in the field. Solid-state nanopore[102,103] and nanogapped electrodes[62] are emerging as the other two versatile and powerful platforms/tools for single (bio)molecule studies. P-engineering of single solid-state nanopore with Au decoration would render nanopores additional plasmonic properties and functions for potential useful bioapplications. Further technological challenges include the integration of nanopore or nanogapped electrodes into nanofludics for label-free single-molecule sensing and sequencing,[104] the incorporation of plasmon nano-optical tweezers[78] with (3D) p-rulers[40–41] for manipulating and sensing of single biomolecules, and the creation of new bioimaging modality[37,39] and integrating them with real-life clinic settings and applications, etc. Future advances require continued innovations by chemists in close collaboration with experts in biological and medical fields, and will lead to a new 'Golden Age' of biomedical nanotechnology.[119] Numerous cancer or other disease-related deaths could be averted in the near future, and our lives will be finally shaped by the advances and developments in the fields.

Acknowledgements

This work was supported by start-up funds from the Changchun Institute of Applied Chemistry of Chinese Academy of Sciences, the National Science Foundation of China (no. 21175125), and the State Key Laboratory of Electroanalytical Chemistry (no. 110000R387).

Received: February 13, 2012
Published online:

[1] M.-C. Daniel, D. Astruc, *Chem. Rev.* **2004**, *104*, 293.
[2] N. L. Rosi, C. A. Mirkin, *Chem. Rev.* **2005**, *105*, 1547.
[3] M. Hu, J. Y. Chen, Z.-Y. Li, L. Au, G. V. Hartland, X. D. Li, M. Marquez, Y. N. Xia, *Chem. Soc. Rev.* **2006**, *35*, 1084.
[4] P. K. Jain, X. H. Huang, I. H. El-Sayed, M. A. El-Sayed, *Acc. Chem. Res.* **2008**, *41*, 1578.
[5] E. Boisselier, D. Astruc, *Chem. Soc. Rev.* **2009**, *38*, 1759.
[6] D. A. Giljohann, D. S. Seferos, W. L. Daniel, M. D. Massich, P. C. Patel, C. A. Mirkin, *Angew. Chem. Int. Ed.* **2010**, *49*, 3280.
[7] E. C. Dreaden, M. A. Mackey, X. H. Huang, B. Kang, M. A. El-Sayed, *Chem. Soc. Rev.* **2011**, *40*, 3391.
[8] C. M. Cobley, J. Y. Chen, E. C. Cho, L. H. V. Wang, Y. N. Xia, *Chem. Soc. Rev.* **2011**, *40*, 44.
[9] G. Mie, *Ann. Phys.* **1908**, *25*, 377.
[10] W. P. Faulk, G. M. Taylor, *Immunochemistry* **1971**, *8*, 1081.
[11] M. Fleischmann, P. J. Hendra, A. J. Mcquillan, *Chem. Phys. Lett.* **1974**, *26*, 163.
[12] D. L. Jeanmaire, R. P. Van Duyne, *J. Electroanal. Chem.* **1977**, *84*, 1.
[13] A. Campion, P. Kambhampati, *Chem. Soc. Rev.* **1998**, *27*, 241.
[14] K. A. Willets, R. P. Van Duyne, *Ann. Rev. Phys. Chem.* **2007**, *58*, 267.
[15] X.-M. Qian, S. M. Nie, *Chem. Soc. Rev.* **2008**, *37*, 912.
[16] W. A. Murray, W. L. Barnes, *Adv. Mater.* **2007**, *19*, 3771.
[17] M. E. Stewart, C. R. Anderton, L. B. Thompson, J. Maria, S. K. Gray, J. A. Rogers, R. G. Nuzzo, *Chem. Rev.* **2008**, *108*, 494.
[18] M. B. Cortie, A. M. McDonagh, *Chem. Rev.* **2011**, *111*, 3713.
[19] E. Prodan, C. Radloff, N. J. Halas, P. Nordlander, *Science.* **2003**, *302*, 419.
[20] H. Wang, D. W. Brandl, P. Nordlander, N. J. Halas, *Acc. Chem. Res.* **2007**, *40*, 53.
[21] N. J. Halas, S. Lal, W.-S. Chang, S. Link, P. Nordlander, *Chem. Rev.* **2011**, *111*, 3913.
[22] C. A. Mirkin, R. L. Letsinger, R. C. Mucic, J. J. Storhoff, *Nature.* **1996**, *382*, 607.
[23] R. Elghanian, J. J. Storhoff, R. C. Mucic, R. L. Letsinger, C. A. Mirkin, *Science.* **1997**, *277*, 1078.
[24] T. A. Taton, C. A. Mirkin, R. L. Letsinger, *Science.* **2000**, *289*, 1757.
[25] Y. W. C. Cao, R. C. Jin, C. A. Mirkin, *Science.* **2002**, *297*, 1536.
[26] S.-J. Park, T. A. Taton, C. A. Mirkin, *Science.* **2002**, *295*, 1503.
[27] J.-M. Nam, C. S. Thaxton, C. A. Mirkin, *Science.* **2003**, *301*, 1884.
[28] N. L. Rosi, D. A. Giljohann, C. S. Thatox, A. K. R. Lytton-Jean, M. S. Han, C. A. Mirkin, *Science* **2006**, *312*, 1027.
[29] S. J. Oldenburg, R. D. Averitt, S. L. Westcott, N. J. Halas, *Chem. Phys. Lett.* **1998**, *288*, 243.
[30] L. R. Hirsch, R. J. Stafford, J. A. Bankson, S. R. Sershen, B. Rivera, R. E. Price, J. D. Hazle, N. J. Halas, J. L. West, *Proc. Natl. Acad. Sci. USA* **2003**, *100*, 13549.
[31] I. H. El-Sayed, X. H. Huang, M. A. El-sayed, *Nano Lett.* **2005**, *5*, 829.
[32] X. H. Huang, I. H. El-Sayed, W. Qian, M. A. El-Sayed, *J. Am. Chem. Soc.* **2006**, *128*, 2115.
[33] C.-C. Chen, Y.-P. Lin, C.-W. Wang, H.-C. Tzeng, C.-H. Wu, Y.-C. Chen, C.-P. Chen, L.-C. Chen, Y.-C. Wu, *J. Am. Chem. Soc.* **2006**, *128*, 3709.
[34] J. Y. Chen, D. L. Wang, J. F. Xi, L. Au, A. Siekkinen, A. Warsen, Z.-Y. Li, H. Zhang, Y. N. Xia, X. D. Li, *Nano Lett.* **2007**, *7*, 1318.
[35] M. S. Yavuz, Y. Y. Cheng, J. Y. Chen, C. M. Cobley, Q. Zhang, M. Rycenga, J. W. Xie, C. Kim, A. G. Schwartz, L. H. V. Wang, Y. N. Xia, *Nat. Mater.* **2009**, *8*, 935.
[36] X. M. Qian, X.-H. Peng, D. O. Ansari, Q. Yin-Goen, G. Z. Chen, D. M. Shin, L. Yang, A. N. Young, M. D. Wang, S. M. Nie, *Nat. Biotechnol.* **2008**, *26*, 83.
[37] Y. D. Jin, C. X. Jia, S.-W. Huang, M. O'Donnell, X. H. Gao, *Nat. Commun.* **2010**, *1*, 41.
[38] Y. D. Jin, X. H. Gao, *J. Am. Chem. Soc.* **2009**, *131*, 17774.
[39] W. Wang, K. Foley, X. Shan, X. P. Wang, S. Eaton, V. J. Nagaraj, P. Wiktor, U. Patel, N. J. Tao, *Nat. Chem.* **2011**, *3*, 249.
[40] C. Sönnichsen, B. M. Reinhard, J. Liphardt, A. P. Alivisatos, *Nat. Biotechnol.* **2005**, *23*, 741.
[41] N. Liu, M. Hentschel, T. Weiss, A. P. Alivisatos, H. Giessen, *Science* **2011**, *332*, 1407.
[42] P. Kohli, C. C. Harrell, Z. H. Cao, R. Gasparac, W. H. Tan, C. R. Martin, *Science* **2004**, *305*, 984.

[43] J. F. Li, Y. F. Huang, Y. Ding, Z. L. Yang, S. B. Li, X. S. Zhou, F. R. Fan, W. Zhang, Z. Y. Zhou, D. Y. Wu, B. Ren, Z. L. Wang, Z. Q. Tian, *Nature* **2010**, *464*, 392.
[44] A. J. Haes, R. P. Van Duyne, *J. Am. Chem. Soc.* **2002**, *124*, 10596.
[45] W. H. Zhang, L. N. Huang, C. Santschi, O. J. F. Martin, *Nano Lett.* **2010**, *10*, 1006.
[46] M. De, P. S. Ghosh, V. M. Rotello, *Adv. Mater.* **2008**, *20*, 4225.
[47] X. H. Huang, S. Neretina, M. A. El-Sayed, *Adv. Mater.* **2009**, *21*, 4880.
[48] S. Lal, S. E. Clare, N. J. Halas, *Acc. Chem. Res.* **2008**, *41*, 1842.
[49] R. Bardhan, S. Lal, A. Joshi, N. J. Halas, *Acc. Chem. Res.* **2011**, *44*, 936.
[50] D.-K. Lim, K.-S. Jeon, J.-H. Hwang, H. Kim, S. Kwon, Y. D. Suh, J.-M. Nam, *Nat. Nanotechnol.* **2011**, *6*, 452.
[51] K.-W. Hu, T.-M. Liu, K.-Y. Chung, K.-S. Huang, C.-T. Hsieh, C.-K. Sun, C.-S. Yeh, *J. Am. Chem. Soc.* **2009**, *131*, 14186.
[52] M. J. Banholzer, N. Harris, J. E. Millstone, G. C. Schatz, C. A. Mirkin, *J. Phys. Chem. C* **2010**, *114*, 7521.
[53] Y. D. Jin, X. H. Gao, *Nat. Nanotechnol.* **2009**, *4*, 571.
[54] T. S. Troutman, S. J. Leung, M. Romanowski, *Adv. Mater.* **2009**, *21*, 2334.
[55] J.-W. Kim, E. I. Galanzha, E. V. Shashkov, H.-M. Moon, V. P. Zharov, *Nat. Nanotechnol.* **2009**, *4*, 688.
[56] S. S. Acimovic, M. P. Kreuzer, M. U. González, R. Quidant, *ACS Nano* **2009**, *3*, 1231.
[57] B. J. Y. Tan, C. H. Sow, T. S. Koh, K. C. Chin, A. T. S. Wee, C. K. Ong, *J. Phys. Chem. B* **2005**, *109*, 11100.
[58] E. M. Larsson, J. Alegret, M. Käll, D. S. Sutherland, *Nano Lett.* **2007**, *7*, 1256.
[59] M. Hentschel, D. Dregely, R. Vogelgesang, H. Giessen, N. Liu, *ACS Nano* **2011**, *5*, 2042.
[60] N. Liu, T. Weiss, M. Mesch, L. Langguth, U. Eigenthaler, M. Hirscher, C. Sönnichsen, H. Giessen, *Nano Lett.* **2010**, *10*, 1103.
[61] J. Mcphillips, A. Murphy, M. P. Jonsson, W. R. Hendren, R. Atkinson, F. Höök, A. Zayats, R. J. Pollard, *ACS Nano* **2010**, *4*, 2210.
[62] T. Li, W. P. Hu, D. B. Zhu, *Adv. Mater.* **2010**, *22*, 286.
[63] X. Wang, C. S. Ozkan, *Nano Lett.* **2008**, *8*, 398.
[64] A. V. Kabashin, P. Evans, S. Pastkovsky, W. Hendren, G. A. Wurtz, R. Atkinson, R. Pollard, V. A. Podolskiy, A. V. Zayats, *Nat. Mater.* **2009**, *8*, 867.
[65] R. Wei, D. Pedone, A. Zürner, M. Döblinger, U. Rant, *Small* **2010**, *6*, 1406.
[66] A. A. Yanik, A. E. Cetin, M. Huang, A. Artar, S. H. Mousavi, A. Khanikaev, J. H. Connor, G. Shvets, H. Altug, *Proc. Natl. Acad. Sci. USA* **2011**, *108*, 11784.
[67] A. Wijaya, S. B. Schaffer, I. G. Pallares, K. Hamad-Schifferli, *ACS Nano* **2009**, *3*, 80.
[68] D. Kagan, R. Laocharoensuk, M. Zimmerman, C. Clawson, S. Balasubramanian, D. Kong, D. Bishop, S. Sattayasamitsathit, L. F. Zhang, J. Wang, *Small* **2010**, *6*, 2741.
[69] R. Weissleder, *Nat. Biotechnol.* **2001**, *19*, 316.
[70] P. K. Jain, W. Y. Huang, M. A. El-Sayed, *Nano Lett.* **2007**, *7*, 2080.
[71] J. A. Fan, C. H. Wu, K. Bao, J. M. Bao, R. Bardhan, N. J. Halas, V. N. Manoharan, P. Nordlander, G. Shvets, F. Capasso, *Science* **2010**, *328*, 1135.
[72] M. Hentschel, M. Saliba, R. Vogelgesang, H. Giessen, A. P. Alivisatos, N. Liu, *Nano Lett.* **2010**,*10*, 2721.
[73] S. Link, M. A. El-Sayed, *Annu. Rev. Phys. Chem.* **2003**, *54*, 331.
[74] X. D. Wang, Y. J. Pang, G. Ku, X. Y. Xie, G. Stoica, L. H. V. Wang, *Nat. Biotechnol.* **2003**, *21*, 803.
[75] Y. W. Wang, X. Y. Xie, X. D. Wang, G. Ku, K. L. Gill, D. P. O'Neal, G. Stoica, L. H. V. Wang, *Nano Lett.* **2004**, *4*, 1689.
[76] X. M. Yang, S. E. Skrabalak, Z.-Y. Li, Y. N. Xia, L. H. V. Wang, *Nano Lett.* **2007**, *7*, 3798.
[77] E. I. Galanzha, E. V. Shashkov, T. Kelly, J.-W. Kim, L. Yang, V. P. Zharov, *Nat. Nanotechnol.* **2009**, *4*, 855.
[78] M. L. Juan, M. Righini, R. Quidant, *Nat. Photonics* **2011**, *5*, 349.
[79] G. Volpe, R. Quidant, G. Badenes, D. Petrov, *Phys. Rev. Lett.* **2006**, *96*, 238101.
[80] K. Wang, E. Schonbrun, P. Steinvurzel, K. B. Crozier, *Nat. Commun.* **2011**, *2*, 469.
[81] A. E. Nel, L. Mädler, D. Velegol, T. Xia, E. M. V. Hoek, P. Somasundaran, F. Klaessig, V. Castranova, M. Thompson, *Nat. Mater.* **2009**, *8*, 543.
[82] M. R. Dreher, W. G. Liu, C. R. Michelich, M. W. Dewhirst, F. Yuan, A. Chilkoti, *J. Natl. Cancer Inst.* **2006**, *98*, 335.
[83] H. S. Choi, W. Liu, P. Misra, E. Tanaka, J. P. Zimmer, B. I. Ipe, M. G. Bawandi, J. Frangioni, *Nat. Biotechnol.* **2007**, *25*, 1165.
[84] B. D. Chithrani, A. A. Ghazani, W. C. W. Chan, *Nano Lett.* **2006**, *6*, 662.
[85] E. Jing, B. S. Kim, J. T. Rutka, W. C. W. Chan, *Nat. Nanotechnol.* **2008**, *3*, 145.
[86] Y. Pan, S. Neuss, A. Leifert, M. Fischler, F. Wen, U. Simon, G. Schmid, W. Brandau, W. Jahnen-Dechent, *Small* **2007**, *3*, 1941.
[87] E. C. Cho, L. Au, Q. Zhang, Y. N. Xia, *Small* **2010**, *6*, 517.
[88] D.-K. Lim, K.-S. Jeon, H. M. Kim, J.-M. Nam, Y. D. Suh, *Nat. Mater.* **2010**, *9*, 60.
[89] A. Louie, *Chem. Rev.* **2010**, *110*, 3146.
[90] R. Weissleder, *Nat. Rev. Cancer.* **2002**, *2*, 11.
[91] R. Bardhan, W. X. Chen, C. Perez-Torres, M. Bartels, R. M. Huschka, L. L. Zhao, E. Morosan, R. G. Pautler, A. Joshi, N. J. Halas, *Adv. Funct. Mater.* **2009**, *19*, 3901.
[92] J. Cheon, J.-H. Lee, *Acc. Chem. Res.* **2008**, *41*, 1630.
[93] A. Verma, O. Uzun, Y. H. Hu, Y. Hu, H.-S. Han, N. Watson, S. Chen, D. J. Irvine, F. Stellacci, *Nat. Mater.* **2008**, *7*, 588.
[94] X. N. Shan, U. Patel, S. P. Wang, R. Iglesias, N. J. Tao, *Science* **2010**, *327*, 1363.
[95] B. Kim, G. Han, B. Toley, C.-K. Kim, V. M. Rotello, N. S. Forbes, *Nat. Nanotechnol.* **2010**, *5*, 465.
[96] C. Kim, S. S. Agasti, Z. J. Zhu, L. Isaacs, V. M. Rotello, *Nat. Chem.* **2010**, *2*, 962.
[97] L. R. Hirsch, A. M. Gobin, A. R. Lowery, F. Tam, R. A. Drezek, N. J. Halas, J. L. West, *Ann. Biomed. Eng.* **2006**, *34*, 15.
[98] J. N. Anker, W. P. Hall, O. Lyandres, N. C. Shan, J. Zhao, R. P. Van Duyne, *Nat. Mater.* **2008**, *7*, 442.
[99] N. Liu, M. Mesch, T. Weiss, M. Hentschel, H. Giessen, *Nano Lett.* **2010**, *10*, 2342.
[100] S. Chen, M. Svedendahl, R. P. Van Duyne, M. Käll, *Nano Lett.* **2011**, *11*, 1826.
[101] Z. Siwy, L. Trofin, P. Kohli, L. A. Baker, C. Trautmann, C. R. Martin, *J. Am. Chem. Soc.* **2005**, *127*, 5000.
[102] C. Dekker, *Nat. Nanotechnol.* **2007**, *2*, 209.
[103] S. Howorka, Z. Siwy, *Chem. Soc. Rev.* **2009**, *38*, 2360.
[104] M. Tsutsui, S. Rahong, Y. Lizumi, T. Okazaki, M. Taniguchi, T. Kawai, *Sci. Rep.* **2011**, *1*, 46.
[105] Y. Cui, Q. Q. Wei, H. K. Park, C. M. Lieber, *Science* **2001**, *293*, 1289.
[106] E. S. Forzani, H. Q. Zhang, L. A. Nagahara, I. Amlani, R. Tsui, N. J. Tao, *Nano Lett.* **2004**, *4*, 1785.

Adv. Mater. **2012**,
DOI: 10.1002/adma.201200622

[107] B. Q. Xu, P. M. Zhang, X. L. Li, N. J. Tao, *Nano Lett.* **2004**, *4*, 1105.
[108] G. L. Liu, Y. D. Yin, S. Kunchakarra, B. Mukherjee, D. Gerion, S. D. Jett, D. G. Bear, J. W. Gray, A. P. Alivisatos, L. P. Lee, F. F. Chen, *Nat. Nanotechnol.* **2006**, *1*, 47.
[109] M. D. Porter, R. J. Lipert, L. M. Siperko, G. Wang, R. Narayanana, *Chem. Soc. Rev.* **2008**, *37*, 1001.
[110] G. A. Baker, D. S. Moore, *Anal. Bioanal. Chem.* **2005**, *382*, 1751.
[111] G. Peng, U. Tisch, O. Adams, M. Hakim, N. Shehada, Y. Y. Broza, S. Billan, R. Abdah-Bortnyak, A. Kuten, H. Haick, *Nat. Nanotechnol.* **2009**, *4*, 669.
[112] J. Yang, J. Lee, J. kang, S. J. Oh, H.-J. Ko, J.-H. Son, K. Lee, J.-S. Suh, Y.-M. Huh, S. Haam, *Adv. Mater.* **2009**, *21*, 4339.
[113] A. K. Salem, P. C. Searson, K. W. Leong, *Nat. Mater.* **2003**, *2*, 668.
[114] L. Y. T. Chou, K. Ming, W. C. W. Chan, *Chem. Soc. Rev.* **2011**, *40*, 233.
[115] P. Ghosh, G. Han, M. De, C. K. Kim, V. M. Rotello, *Adv. Drug Deliv. Rev.* **2008**, *60*, 1307.
[116] M. R. Choi, K. J. Stanton-Maxey, J. K. Stanley, C. S. Levin, R. Bardhan, D. Akin, S. Badve, J. Sturgis, J. P. Robinson, R. Bashir, N. J. Halas, S. E. Clare, *Nano Lett.* **2007**, *7*, 3759.
[117] J. Heber, *Nature* **2009**, *461*, 720.
[118] Y. D. Jin, X. F. Kang, Y. H. Song, B. L. Zhang, G. J. Cheng, S. J. Dong, *Anal. Chem.* **2001**, *73*, 2843.
[119] E. C. Dreaden, A. M. Alkilany, X. H. Huang, C. J. Murphy, M. A. El-Sayed, *Chem. Soc. Rev.* **2011**, DOI: 10.1039/c1cs15237h.